JGR Solid Earth

RESEARCH ARTICLE
10.1029/2021JB023848

Peak Frequency Changes From HV Spectral Ratios in Central Italy: Effects of Strong Motions and Seasonality Over 12 Years of Observations

Maurizio Vassallo[1], Giovanna Cultrera[2], Giuseppe Di Giulio[1], Fabrizio Cara[2], and Giuliano Milana[2]

[1]Istituto Nazionale di Geofisica e Vulcanologia, Sezione Roma1, L'Aquila, Italy, [2]Istituto Nazionale di Geofisica e Vulcanologia, Sezione Roma1, Roma, Italy

Key Points:

- H/V frequency peak shows abrupt changes at the occurrence of strong earthquakes
- H/V frequency peak shows changes linked to seasonal variations
- Massive H/V analysis of 12 years of continuous data acquired by two permanent seismic stations operating in the Central Apennines

Supporting Information:

Supporting Information may be found in the online version of this article.

Correspondence to:

M. Vassallo,
maurizio.vassallo@ingv.it

Citation:

Vassallo, M., Cultrera, G., Di Giulio, G., Cara, F., & Milana, G. (2022). Peak frequency changes from HV spectral ratios in Central Italy: Effects of strong motions and seasonality over 12 years of observations. *Journal of Geophysical Research: Solid Earth*, *127*, e2021JB023848. https://doi.org/10.1029/2021JB023848

Received 16 DEC 2021
Accepted 29 APR 2022

Author Contributions:

Conceptualization: Maurizio Vassallo
Data curation: Maurizio Vassallo
Formal analysis: Giovanna Cultrera, Giuseppe Di Giulio, Fabrizio Cara
Methodology: Maurizio Vassallo, Giuseppe Di Giulio
Software: Maurizio Vassallo
Supervision: Giovanna Cultrera
Validation: Maurizio Vassallo, Giovanna Cultrera, Giuseppe Di Giulio, Fabrizio Cara
Writing – original draft: Maurizio Vassallo, Giovanna Cultrera, Giuseppe Di Giulio, Giuliano Milana

Abstract We analyzed 12 years of continuous seismic data acquired by two seismic stations in Central Apennines (Italy) with the aim to investigate the temporal variations of H/V spectral ratios. The two stations are located in the epicentral areas of the main strong motion earthquakes occurred in Central Italy in the last 12 years (L'Aquila 06 April 2009, Mw 6.1; Amatrice 24 August 2016, Mw 6.0; Visso 26 October 2016, Mw 5.9, and Norcia 30 October 2016, Mw 6.5). H/V ratios are computed both on continuous and earthquakes data recorded by the two stations. H/V ratios are subjected to abrupt changes after strong earthquakes. The results highlight that after strong shaking, there are remarkable drops of the peak frequencies (7%–10% of reduction). After this sudden decrease, the peak frequency slowly recovers to the initial value in a time ranging from a few months to a few years. We also observe a moderate frequency variation (of order of 2%–3%) linked to seasonal variations: the peak frequencies increase in the spring-summer months and decrease during the winter. The frequency changes after strong earthquakes have been interpreted in terms of velocity variations of the shallow layers. This effect must be taken into account for microzonation, geophysical, and engineering studies that are often carried out in the epicentral areas after strong earthquakes. H/V analysis over time proved to be a useful procedure for highlighting temporal changes relating to the properties of shallow layers of the propagation medium and could provide relevant information for the site characterization of permanent seismic stations.

Plain Language Summary Permanent seismic stations record the continuous vibrations of the ground and occasionally, they detect earthquake signals. Two Italian stations are located in the epicentral areas where the main earthquakes occurred in Central Italy in the last 12 years. Their data have been used to verify if changes on shallow-soil properties occur after a strong earthquake shaking. The indicator used for the analysis is the frequency at which the soil below the stations amplifies the vibration signal. We found that the frequency value measured at the two stations suddenly decreased by about 7%–10% during the mainshocks and resumed its original value after a few months to years. We also observed small seasonal variation with an increase of the value in spring-summer and a decrease in winter times. The observed changes are most probably caused by the temporal changes of the seismic-wave velocity of the shallow soil. This observation should be accounted for studying the soil properties and for engineering evaluation of the possible effect on buildings.

1. Introduction

The Horizontal-to-Vertical Spectral Ratio (hereinafter H/V) technique is a very popular tool to retrieve information about the shallow-subsoil seismic properties by single-station measurements. This method is widely used in geophysical investigations especially applied to ambient vibration data as a tool for a quick detection of the shear-wave resonance frequency. The technique, originally proposed by Nogoshi and Igarashi (1971) and subsequently widely applied by Nakamura (1989), consists in estimating the ratio between the Fourier amplitude spectra (FAS) of the horizontal (H) to vertical (V) components of ambient noise vibrations or earthquake coda waves recorded at one single station.

The two main advantages of the method, especially if applied to the seismic noise, are the rapidity and the use of single-station measurements that make it low cost and easy to apply (Cultrera et al., 2021). The technique is typically applied in microzonation studies and in the investigation of local site responses (Albarello et al., 2011; Bour et al., 1998; Milana et al., 2020). The H/V noise spectral ratio can provide the fundamental resonance frequency (f0) of the site (Field & Jacob, 1995; Parolai et al., 2004) and, depending on the soil structure and in simple (1D) geological conditions, also the higher harmonics, especially if applied to earthquake data rather than noise. In any

Writing – review & editing: Maurizio Vassallo, Giovanna Cultrera, Giuseppe Di Giulio, Fabrizio Cara, Giuliano Milana

case, Haghshenas et al. (2008) and Cultrera et al. (2014) stressed the absence of correlation between the H/V peak amplitude and the real site amplification estimated through site-to-reference spectral ratios.

Molnar et al. (2018) showed a recent state-of-the-art review of the H/V method, including a discussion on the theoretical basis behind it. The interpretations of the H/V noise ratios are related to different assumptions about the wavefield composition of ambient vibrations. In fact, some authors consider the predominance of body waves (Herak, 2008; Nakamura, 2019), others of surface Rayleigh waves (Fäh et al., 2001), or some proportion of Rayleigh and Love waves (Arai & Tokimatsu, 2004; Endrun, 2011). Another approach on the seismic noise composition is based on the Diffuse Field Approach (Garcia-Jerez et al., 2011, 2012; Piña-Flores et al., 2016; Sánchez-Sesma, 2017), which invokes the Green's functions to link the H/V spectral ratios and the properties of the propagation media. More realistically, the wavefield is a mix of several types of waves and the efforts of the research are toward a complete H/V modeling, for example, considering the entire noise wavefield (Lontsi et al., 2015; Lunedei & Albarello, 2010; Lunedei & Malischewsky, 2015). Due to the large popularity of the technique, some practical guidelines have been drawn up, intended for field experiment design, data processing, and interpretation of the results (SESAME, 2005 user guidelines; Picozzi et al., 2005; Hunter & Crow, 2012; Molnar et al., 2018). These works provide recommendations that should be taken into account in studies based on the H/V spectral ratio technique, trying to lead the users toward a valid data acquisition and a correct choice of the parameters to be used in the analysis, and with an indication for evaluating the robustness of the results and their correct interpretation. In particular, important conditions for obtaining reliable results are the duration of the recordings and the time stability of the results. The record duration is crucial in temporary measurements and must be determined taking into account the expected resonance frequency of the sites. SESAME. (2005) guidelines recommend at least 200 cycles of resonant period for the whole record duration. Moreover, the transient signals (usually associated with specific anthropic sources such as footsteps, traffic cars, machines with moving parts, etc.) should be removed from the processed signal as they could bias the results (SESAME, 2005 guidelines). In the presence of anthropic noise, it is then necessary to have a longer recording duration to achieve reliable estimates.

Concerning the stability of H/V results over time, this issue is affordable only with the availability of very long time recordings. This is the case of the permanent stations of modern seismological networks that record the data continuously. Therefore, it is possible to compute the H/V function on continuous recordings that can include several years of data. Unfortunately, the H/V analysis over time is still not carried out routinely and is performed only in a few and peculiar cases. For example, temporal variations of the H/V ratios have been investigated for monitoring the permafrost active layer seasonal variability (Köhler & Weidle, 2019; Kula et al., 2018) and for monitoring the rock masses stability (Colombero et al., 2018). Lotti et al. (2018) observed H/V temporal variations using 7-month passive seismic data acquired in the Torgiovannetto quarry (near the town of Assisi, Central Italy) in an area threatened by a rockslide. The H/V monitoring revealed changes of subsoil site conditions that could affect the stability of the rockslide. This work also suggests that in general the H/V monitoring can give useful information on seismic site response studies. La Rocca et al. (2020) analyzed the time stability of H/V spectral ratios for sites located in Southern Apennine (Italy) and observed a temporal variability of results for all the stations located near or on topographic heights (on mountains, ridges, or foothills).

In the previous studies, the H/V ratio technique was applied to seismic noise, but in other papers, it was also applied to strong-motion data in order to verify the occurrence of resonant frequency changes.

This kind of approach was proposed by some studies in Japan after very strong earthquakes (Sawazaki et al., 2006; Wu & Peng, 2011, 2012) on some borehole stations of the Japanese strong Motion Network (KiK-Net, https://www.kyoshin.bosai.go.jp/kyoshin/docs/overview_kyoshin_index_en.html). In this case, they did not use the H/V spectral ratios, but they computed the spectral ratios of horizontal components between surface and depth stations. Regardless of some differences in the procedures, these studies obtained similar results, for example, a clear reduction of the peak frequency (30%–70%) at the investigated sites after the occurrence of the mainshocks, followed by a loga rhythmically recovery to the pre-event value. Moreover, Wu and Peng (2011, 2012) also observed a recovery characterized by two stages, the first phase being very rapid (within several hundred seconds to several hours), and the second being slow with recovery lasting more than 5 months.

Despite these encouraging scientific papers, a comprehensive study that uses the ambient seismic noise continuously recorded by permanent seismic stations to monitor the variations of the H/V spectral ratios at the occurrence

of strong earthquakes is still missing. The aim of this study is to investigate the temporal variability of H/V results in Italy, taking advantage of 12-year-long continuous data recorded by two seismic stations of the Italian permanent network (Rete Sismica Nazionale, hereinafter RSN; INGV Seismological Data Centre, 2006, and Margheriti et al., 2021) run by Istituto Nazionale di Geofisica e Vulcanologia (INGV). The two seismic stations are deployed in the Central Apennines area that between 2008 and 2020 was affected by several strong earthquakes, in particular the L'Aquila earthquake of 2009 and the Central Italy (Amatrice, Visso, Norcia, 2016) sequences.

After presenting the seismic stations and the data selected for this study, we discuss the processing used for the H/V analysis on both noise and earthquakes and we describe different tests performed to evaluate the robustness of the obtained results. Then, we study the temporal variations of H/V frequency peaks by correlating them with the meteorological conditions near the seismic stations and at the occurrence of strong earthquakes. We finally discuss the frequency peak variation after strong shaking in terms of property changes of soil.

2. Seismological and Meteorological Data

The analysis was performed on the velocity recordings of two permanent seismic stations (Figure 1 and Table 1) of RSN Italian network: AQU (MN network, MedNet Project Partner Institutions, 1990) and NRCA (IV network). They were selected because of the availability of 12-year-long continuous recordings, including the strong-motion signals of the largest seismic sequences that occurred in Italy since 2009.

Both stations are located in Central Apennines, one of the most active seismic regions in Italy characterized by normal faulting events. The seismicity distribution in Figure 1 and Table 2 shows that from 2009 to 2017, the active faults in Central Italy have caused ruptures for a total extension of more than 100 km along the Apennine direction.

AQU station (Figure 1 and Table 1) is installed on the underground floor (15 m from the ground level) of a stone fortress castle of the 16th century in downtown L'Aquila (Abruzzo region). L'Aquila sits on a fluvial terrace on the left bank of the Aterno River, about 2 km apart from the epicenter of the 6 April 2009, L'Aquila earthquake (Mw 6.1). The mainshock ruptured an ∽16 km long normal fault (Cirella et al., 2012) and nucleated at a depth of about 9 km; it was preceded and followed by a seismic sequence lasting for several months (Table 2 and Figure 1; Chiaraluce et al., 2010). During the earthquake, the town itself and its surroundings suffered severe damage (macroseismic intensity of VIII-IX; Galli & Camassi, 2009; Tertulliani et al., 2011) with 309 fatalities and collapses of many residential buildings and significant damage of many historical monuments (Brandoniosio et al., 2013).

The second station, NRCA (Figure 1 and Table 1), is installed at the ground surface level in a hamlet close to the village of Norcia (Umbria region) and about 60 km NW far from AQU. It is also about 5 km far from the epicenter of the 30 October 2016, Norcia earthquake (Mw 6.5), which caused significant ground-surface coseismic rupture for about 5 km in the proximity of the Monte Vettore fault system, on the border between Marche and Umbria regions (Civico et al., 2018). The Mw 6.5 is the largest mainshock of the seismic sequence that hit Central Italy in 2016–2017 (Improta et al., 2019) and started on 24 August 2016, with an Mw 6.0 event, followed by major earthquakes in a vast area. In January 2017, many of the epicenters of the sequence were located up to 20 km North of L'Aquila (Figure 1 and Table 2). Many historical villages were severely struck (Galli et al., 2017; Rossi et al., 2019), such as Amatrice and Arquata del Tronto, whose downtowns were completely destroyed (Rossi et al., 2019).

The site responses at both AQU and NRCA stations are known fairly well because of the microzonation studies following the 2009 and 2016–2017 seismic emergencies (Albarello et al., 2011 and Milana et al., 2011 for AQU; Priolo et al., 2020 and Amanti et al., 2020 for NRCA). Additional information on local soil properties is also provided by national projects dedicated to the characterization of the Italian strong motion stations (Cultrera et al., 2018), and by research papers focused on the seismic response of the epicentral area (Bordoni et al., 2014; Pagliaroli et al., 2019; among many others). The geophysical and geological information for NRCA (Working group INGV, 2018a and 2018b) and AQU can be downloaded from the INGV database for the site characterization of the permanent seismic stations (http://crisp.ingv.it) and from both the Italian Accelerometric Archive (ITACA, http://itaca.mi.ingv.it/, Russo et al., 2022, D'Amico et al., 2020 and Luzi et al., 2008) and the Engineering Strong-motion database (ESM, https://esm.mi.ingv.it, Luzi et al., 2016). According to these

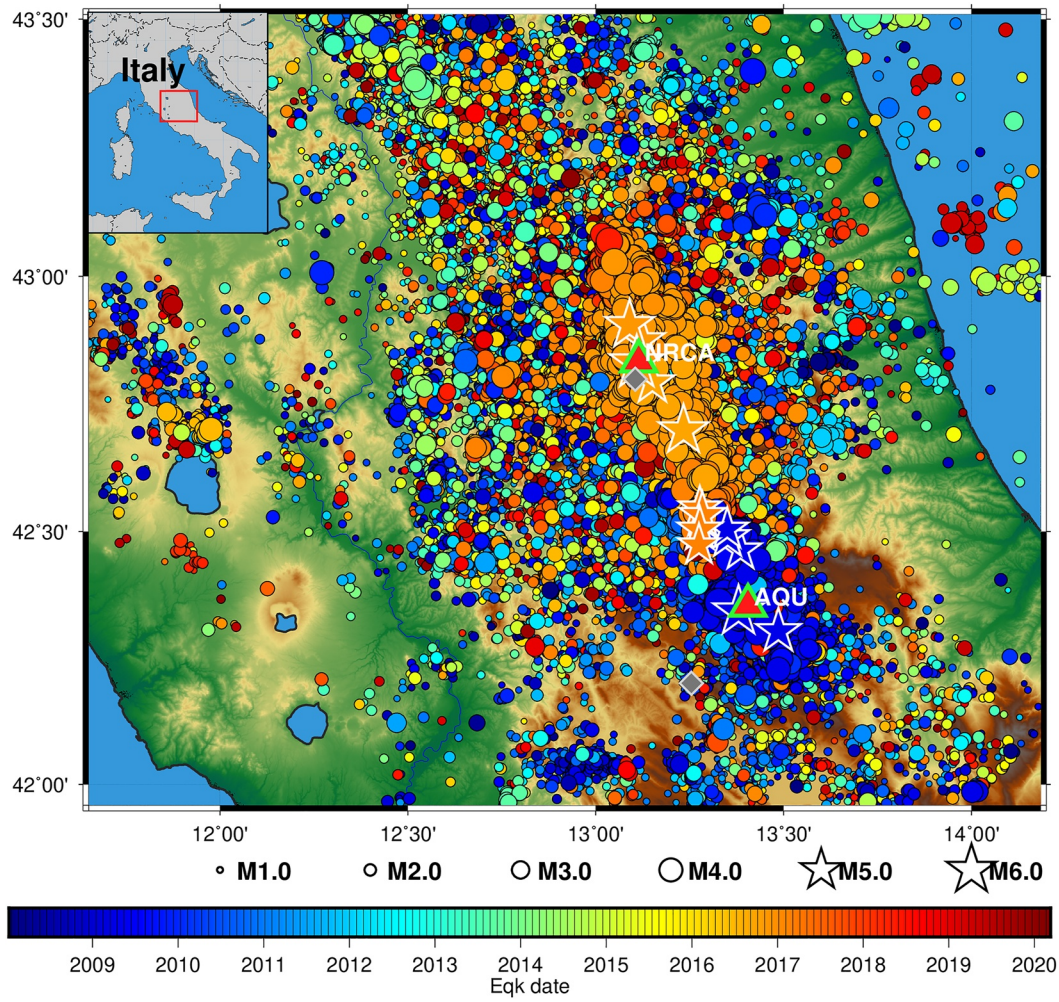

Figure 1. Map of central Italy with epicenters of the earthquakes (circles and stars), seismic (red triangles, AQU and NRCA), and meteorological stations (gray diamond) used in this study. Earthquake locations span from 01 January 2008 to 31 January 2020 and include magnitude (ML or Mw) in the range 1.0–6.5 (circle size proportional to magnitude, stars refer to M ≥ 5). The color scale of the epicenters represents the origin time of seismic events (about 160,000). The spatial and temporal concentrations of events highlight the strongest seismic sequences of the area: L'Aquila earthquake of 2009 (blue) and Central Italy 2016–2017 (orange).

websites, the resonance frequency (f0) at the two target stations was computed through the H/V spectral ratio on a few hours of noise and on earthquake recordings (at least 100 events).

The f0 value of AQU reported in ITACA or ESM archives is 0.56 Hz from noise measurements, whereas H/V on earthquakes shows a broad peak centered at about 0.49 Hz. We believe that the different value of f0 between noise and earthquakes is not statistically significant considering the disparity in the H/V computation. Indeed, in the abovementioned databases, the H/V of noise was computed on FAS and window length of 50 s, whereas the H/V of earthquake was computed on response spectra with different window lengths using a large group of different events (397 earthquakes with a magnitude ranging from 3 to 6.5 and an epicentral distance from 1 to 335 km). This low-frequency resonance is related to the presence of a seismic interface at about 300 m depth, where silt quaternary deposits are overimposed to limestone and sandstone of the Aterno river basin (Bordoni et al., 2014). Besides the low-frequency resonance at AQU, the H/V ratios show broad and multiple peaks with comparable amplitudes in the frequency band 2–5 Hz (Figure 2) that are connected to the presence of other velocity contrasts. Another peak above 10 Hz is probably related to a shallow velocity contrast although qualitative geological considerations on the materials (heterometric calcareous breccias) suggest that the shear-wave velocity can be relatively high (vs. >400 m) soon below the station. The near-surface part of AQU subsoil model

Table 1
Main Characteristics of the Seismic (http://terremoti.ingv.it/en/instruments, Last Accessed in April 2020) and Meteorological (https://servizioidrografico.regione.umbria.it and https://www.regione.abruzzo.it/content/servizio-idrografico-mareografico; Last Accessed in July 2020) Stations

Station (Network)	Data type	Analyzed period	Lat (°)	Lon. (°)	Elevation (m)
AQU (MN)	Seismic velocity (STRECKEISEN STS2 - flat response from 120 s to 10 Hz) and acceleration (Episensor FBA-ES-T); GAIA acquisition system	19 Febuary 2008–31 January 2020[a]	42.354	13.405	710
NRCA (IV)	Seismic velocity (Nanometrics Trillium 40s—flat response from 40 s to 50 Hz) and acceleration (Episensor FBA-ES-T); Quanterra Q730 digitizer (changed with a Q330 from 01/03/2019)	24 November 2008–31 January 2020[b]	42.834	13.114	927
NRC (IT)	Acceleration (BARTEC SYSCOM MS2007+); Reftek 130 digitizer	24 November 2008–31 January 2020[c]	42.793	13.096	616
NORCIA	Temperature and rain meteorological data	01 January 2008–31 January 2020	42.799	13.105	700
L'AQUILA	Temperature and rain meteorological data	01 January 2008–31 January 2020	42.200	13.254	590

[a]In the period 31 December 2017–01 March 2019, the station was not working for technical problems. [b]Accelerometric recordings of many mainshocks are missing during the considered period. [c]Data used only for PGV estimates recorded during mainshocks.

consists of calcareous breccias with an average Vs of about 800 m/s and thickness ranging between 15 and 50 m. Although 2D geological models are available for L'Aquila (Macerola et al., 2019), a velocity profile obtained through specific geophysical surveys for the site of AQU is missing. Indeed, the average shear-wave velocity in the uppermost 30 m (V_{S30}) reported in ESM database (598 m/s) was derived from a terrain-based model assuming a 90-m digital elevation model and topographic and geological proxies (topography class T1, i.e., slope less than 15°, based on the EC8 building code prescriptions; CEN, 2004).

NRCA is characterized by a higher resonance frequency with a single sharp peak in the H/V noise curves at 7.0 Hz and a mean amplitude level of about 5 (Figure 2). The site has a V_{S30} of 590 m/s and the bedrock layer (vs. >800 m/s) is located at a depth of 18 m. The velocity profile obtained through an MASW linear array shows a very thin (about 4–5 m) surface layer with a velocity of about 250 m/s overlaying a faster one with Vs of about 600 m/s. Considering the limited capability of the MASW technique, we cannot exclude the presence of very soft and thin layers in the very first 5 m of the profile that can be responsible for an impedance contrast with the calcareous limestone bedrock (vs. of about 1,000 m/s, GEER, 2017; Working group INGV, 2018b) and then causing the observed high-frequency resonance. Although the topography class of NRCA is the same of AQU (EC8 building code is T1), it approaches the upper limit of the class because it is characterized by a slope of 14°.

With the aim of studying the effect of weather conditions on seismic recordings at the two stations, we also used raw meteorological data (temperature and rainfall) recorded from January 2008 to January 2020 at two meteorological stations, NORCIA and L'AQUILA, close to the seismological ones (Table 1 and diamond symbols in Figure 1): NORCIA is close to NRCA (about 4 km S-SW) and it belongs to the hydrographic service of the Umbria Region (https://servizioidrografico.regione.umbria.it), whereas the L'AQUILA meteorological station is at about 20 km SW from AQU and it belongs to Territory-Environment Department of the Abruzzo region (Civil Protection Activities Planning Service, Hydrographic and Oceanographic Office, https://www.regione.abruzzo.it/content/servizio-idrografico-mareografico). Both stations measure rain and temperature by means of a rain gauge and an air thermometer, and the raw data are provided as a daily average in case of NORCIA and as single measurements every 15 minutes for L'AQUILA.

3. Spectral Ratio Analysis on Continuous Data

We analyzed 12 years of continuous seismological data from 2008 to early 2020, recorded at NRCA and AQU (Table 1) and stored in the European Integrated Data Archive (EIDA, https://eida.ingv.it last accessed in April 2022; Strollo et al., 2021). The analysis has been performed on velocimetric data with a sampling frequency of 20 sps (BH stream as provided by EIDA archive) to optimize the computation speed.

Table 2
List of the Largest Earthquakes (Mw ≥ 5.0) of the Two Seismic Sequences (2009 and 2016–2017) in Central Italy, and Epicentral Distance (Repi), Azimuth and Peak Ground Velocity and Acceleration (PGV and PGA, Respectively) Experienced at Stations AQU, NRCA, and NRC, When Available

#	Earthquake date and time	Lat. (°)	Lon. (°)	Depth (km)	Mw	Location	Recording station	Repi (km)	Azimuth (°)	PGV (m/s)	PGA (m/s2)
1	06 April 2009_01:32	42.342	13.380	8.3	6.1	L'Aquila earthquake, 2 km SW L'Aquila (AQ)	AQU	2	234	0.290	3.06
2	06 April 2009_23:15	42.463	13.385	9.7	5.1	8 km E Pizzoli (AQ)	AQU	12	353	0.020	0.38
3	07 April 2009_17:47	42.303	13.486	17.1	5.5	1 km N Fossa (AQ)	AQU	9	129	0.050	0.71
4	09 April 2009_00:52	42.489	13.351	11.0	5.4	5 km SE Capitignano (AQ)	AQU	16	344	0.020	0.35
5	09 April 2009_19:38	42.504	13.350	9.3	5.0	4 km E Capitignano (AQ)	AQU	17	346	0.007	0.19
6	24 August 2016_01:36	42.698	13.233	8.1	6.0	Amatrice earthquake, 1 km W Accumoli (RI)	AQU	41	340	0.040	0.25
							NRCA	–	–	–	–
							NRC	15	133	0.300	3.67
7	24 August 2016_02:33	42.792	13.151	8.0	5.3	5 km E Norcia (PG)	AQU	53	337	0.015	0.07
							NRCA	–	–	–	–
							NRC	4	91	0.100	1.91
8	26 October 2016_17:10	42.875	13.124	8.1	5.4	3 km SW Castelsantangelo sul Nera (MC)	AQU	62	339	0.004	0.08
							NRCA	–	–	–	–
							NRC	9	14	0.260	2.95
9	26 October 2016_19:18	42.905	13.090	9.6	5.9	Visso earthquake, 3 km S Visso (MC)	AQU	66	340	0.013	0.09
							NRCA	–	–	–	–
							NRC	13	12	0.160	3.66
10	30 October 2016_06:40	42.830	13.109	10	6.5	Norcia earthquake, 4 km NE Norcia (PG)	AQU	58	336	0.060	0.45
							NRCA	–	–	–	–
							NRC	5	15	0.480	4.76
11	18 January 2017_09:25	42.545	13.277	10	5.1	3 km NW Capitignano (AQ)	AQU	24	334	0.008	0.15
							NRCA	–	–	–	–
							NRC	31	152	0.020	0.50
12	18 January 2017_10:14	42.531	13.284	9.6	5.5	2 km NW Capitignano (AQ)	AQU	22	334	0.012	0.21
							NRCA	–	–	–	–
							NRC	33	152	0.020	0.38
13	18 January 2017_10:25	42.503	13.277	9.4	5.4	3 km SW Capitignano (AQ)	AQU	–	–	–	–
							NRCA	–	–	–	–
							NRC	35	155	0.013	0.26
14	18 January 2017_13:33	42.473	13.275	9.5	5.0	2 km N Barete (AQ)	AQU	17	322	0.004	0.11
							NRCA	–	–	–	–
							NRC	38	158	0.013	0.30

In order to evaluate the data quality and to identify any anomalous noise level in the frequency range of interest, we computed the Power Spectral Density (PSD) following the approach proposed by McNamara and Buland (2004). The analysis was performed on the whole data set available at the two stations. For each component, the PSDs were computed in time windows of 3,600 s overlapped at 50% (using the software PPSD of obspy https://github.com/obspy/obspy/wiki/, Megies et al., 2011). The analysis did not reveal any problems in the data, the PSDs varying within the Peterson (1993) curves, which are the standard curves for the seismic background noise spectral level (Bormann & Wielandt, 2013). A further statistical analysis was performed to compute the values of 90th percentiles for the two stations across years. The 90th percentile levels are very similar to each other, except for the years in which the seismic sequences occurred near the two stations, increasing the noise level (Figure S1 in Supporting Information S1).

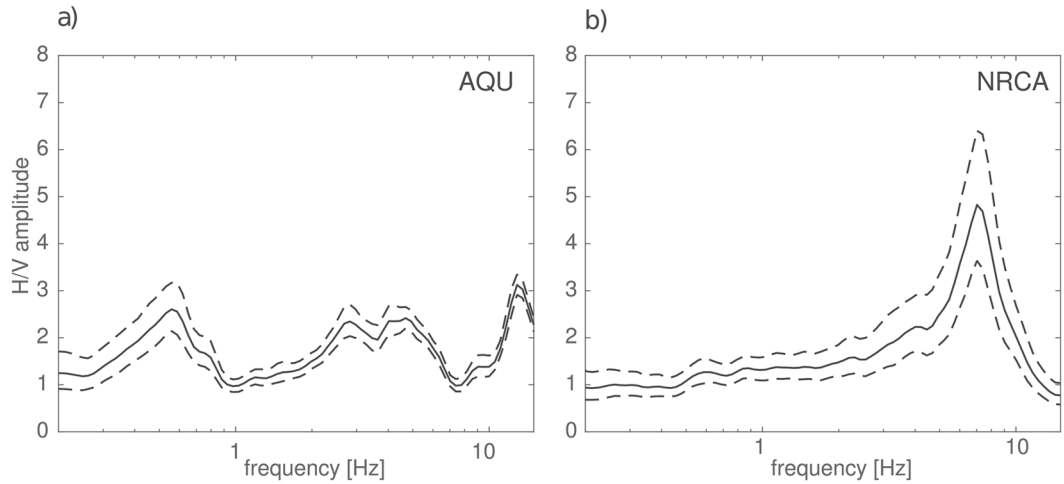

Figure 2. H/V spectral ratio on noise (geometric mean ± 1 standard deviation) for (a) AQU and (b) NRCA computed for one day (12 February 2015 for NRCA and 10 October 2015 for AQU). From CRISP database (http://crisp.ingv.it).

The continuous seismic data have been automatically processed with the Geopsy tool (www.geopsy.org; Wathelet et al., 2020) for the computation of the H/V ratios. After several tests, we have chosen to compute a daily average of H/V obtained by using 60-s-long moving windows without the anti-trigger option (see further considerations on this issue at the end of this section). The 60-s windows were first de-trended (mean and linear trend removal) and tapered at both ends using a cosine function; the FAS were then computed in the frequency band 0.1–10 Hz and smoothed using the Konno-Ohmachi logarithmic window with b value of 40 (Konno & Ohmachi, 1998). The H/Vs for each window were then computed by dividing the horizontal FAS (squared average of the N-S and E-W components of the signal) by the vertical FAS as follows:

$$H/V = \frac{\sqrt{\left[E^2(\omega) + N^2(\omega)\right]/2}}{Z(\omega)}$$

where E(ω), N(ω), and Z(ω) indicate the FAS of East, North, and vertical components, respectively. Finally, the H/V curves are geometrically averaged within each single day.

We tested that the results of our H/V analysis, by using downsampled data at 20 sps (BH stream), are in agreement with the one obtained from the data sampled to 100 sps (HH stream) as shown in Figure S2 in Supporting Information S1.

It is important to highlight that the automatic H/V on the continuous data has been performed considering the entire daily recordings, potentially including both noise and earthquakes. Although the H/V on noise is often similar to the one on earthquakes, sometimes significant differences have been observed (Cultrera et al., 2014; Felicetta et al., 2021). Whenever present, they can be related to energetic waves that are created during earthquakes or to multidimensional effects, for example, in basin environments or topographic reliefs. In order to ensure that these possible differences do not affect the automatic H/V computation, we performed a simple test in which we compare the automatic H/V results (i.e., without anti-trigger) with those obtained through a manual selection of the portion of data to be analyzed. The test was carried out on 10 days of recordings selected over the 12 years in order to have both days with low presence of transient signals and days during seismic sequences characterized by many earthquakes. For these recordings, we manually selected only the time windows not affected by transient signals associated with seismic events and anthropic sources. The selection of noise windows (40–60s long) has been performed also with the help of the anti-trigger algorithm implemented in Geopsy. We then compared the manual and automatic computation of the H/V for the two stations NRCA and AQU: the agreement for all the considered periods is very good with differences well within the corresponding standard deviations (Figure S3 in Supporting Information S1). Therefore, the proposed automatic H/V analysis provides very similar results with respect to the manual one, regardless of earthquakes and transients. We believe that this is due to the very large number of windows used for the noise analysis, which makes the average not sensitive to the transient

signals. In the rest of this paper, we will always refer to the automatic analysis when discussing H/V performed on seismic noise.

Figure 3 shows the H/V curves as a function of frequency and time, computed for the two stations with the automatic procedure and for a period of 12 years (2008–2020). These time analyses allow to investigate the variation of the H/V ratios during many years with special emphasis to the 2009 and 2016–2017 when the L'Aquila and Amatrice-Norcia seismic sequence occurred, respectively. The plot of AQU (Figure 3a) confirms the peaks in the H/V curves at frequencies of about 0.55 Hz and in the range 3–5 Hz (in this range, we consider the peak at 4.3 Hz, which is characterized by the highest amplitude). The first peak at 0.55 Hz appears fairly stable over the 12 years, while the high-peak frequency at 4.3 Hz presents two main temporal variations around its central value. The first temporal variation is clearly seasonal showing a gradual increase and decrease in the peak frequency. On the contrary, the second variation is impulsive and it occurs immediately after the mainshock of L'Aquila (Mw 6.1 of 06 April 2009; Table 2), when the peak frequency abruptly decreases assuming a value of about 3.9 Hz.

The H/V ratios at NRCA station show a clear spectral peak at about 7.3 Hz (Figure 3b) but also temporal variations during the 12 analyzed years. As for AQU station, clear and impulsive drops in the peak frequency are observed several times during the 2016–17 central Italy seismic sequence. Differently from AQU, in this type of representation, the seasonal variations of NRCA peak frequency are not very clear. Figures 3c and 3d show the H/V evolution for AQU and NRCA, respectively, over a more restricted time window. They emphasize what happens at the occurrence of strong earthquakes and several months later when the frequency peaks tend to return to the pre-event value after about 2–3 months for AQU (Figure 3c) and about 16 months (roughly estimated) for NRCA (Figure 3d).

Figure 4 focuses on the peak frequencies (at 4.3 and 7.3 Hz for AQU and NRCA, respectively) following the frequency value trend and their amplitude variation during the 12 years. This kind of graphical representation highlights the two types of frequency variations (seasonal and at occurrence of the main earthquakes) for both stations. Indeed, the peak frequency value increases and decreases periodically following the seasonal variations. Moreover, whenever a strong earthquake occurred near the selected station, we observe clear sharp drops in the peak frequency values. This is particularly evident when we compare the peak frequency trend with the PGV values obtained by integrating the accelerometric data recorded at the stations during the earthquakes of the last 12 years: the decrease in peak frequency is observed at the occurrence of the largest PGV values. The effect on H/V amplitude is less evident with respect to the shift in frequency but our analysis suggests a weak increase in the H/V amplitude especially for NRCA after the Amatrice earthquake (24 August 2016, Mw 6.1) (Figures 3d and 4b). However, interpreting H/V amplitude variation is not easy as it could be related to the vertical component, affected by site response itself and by possibly different nonlinearity effects on the H and V components.

In order to study the seasonal variations of the H/V peak frequency, we investigated the possible correlation with weather conditions, in particular with the temperature (T) and the rainfall (P) measured at meteorological stations very close to the two seismic stations (Figure 1 and Table 1). We first homogenized and smoothed the meteorological data of NORCIA and L'AQUILA stations (temperature T and rainfall P) by producing daily averages and then applying an arithmetic moving average with a 5-day span centered around each day: because we are interested in understanding the long-period variability visible on the H/V frequency peak, this data conditioning does not significantly affect the original time series but smooths the daily variation, which can have a significant temporal and spatial variability. Finally, we compared the temperature and rainfall time series with seismological parameters from H/V noise spectral ratios (peak frequency f and its amplitude A) by calculating a measure of the correlation between two signals in the time-frequency plane and their phase lag. Let us consider 2 time series, one representing T or P meteorological data (x) and the other the H/V frequency peak for its amplitude A (y). We first selected the common time period of x and y and substituted the missing values, if any, with the previous closest measured value. We then computed the continuous wavelet transforms of x and y (Cx and Cy) by using the analytic Morlet wavelet over logarithmic scales with a default value of 12 voices per octave. Finally, we computed the magnitude-squared wavelet coherence in the time-frequency plane as $\frac{|S(C_x^* \cdot C_y)|^2}{[S(|C_x|^2) \cdot S(|C_y|^2)]}$, where S is a smoothing operator in time and scale (see the wcoherence Matlab function for further details: https://it.mathworks.com/help/wavelet/ref/wcoherence.html).

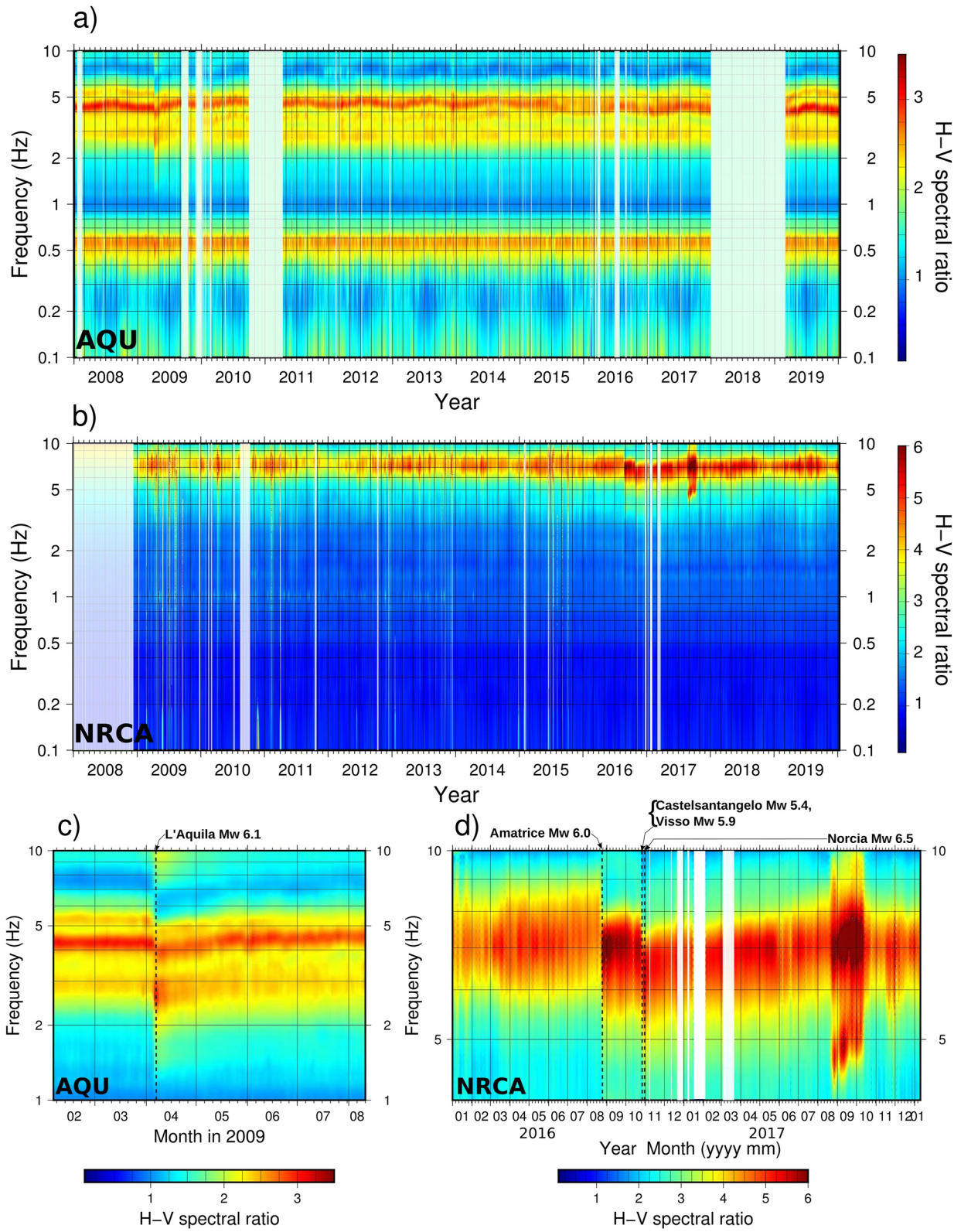

Figure 3. Temporal variation of the H/V ratios computed on continuous data at the two stations for the whole period of 12 years (a), (b) and for a time window around the main shocks (c), (d) (a)–(c) AQU and (b)–(d) NRCA. The vertical black dashed lines show the origin times of main earthquakes that occurred near the stations.

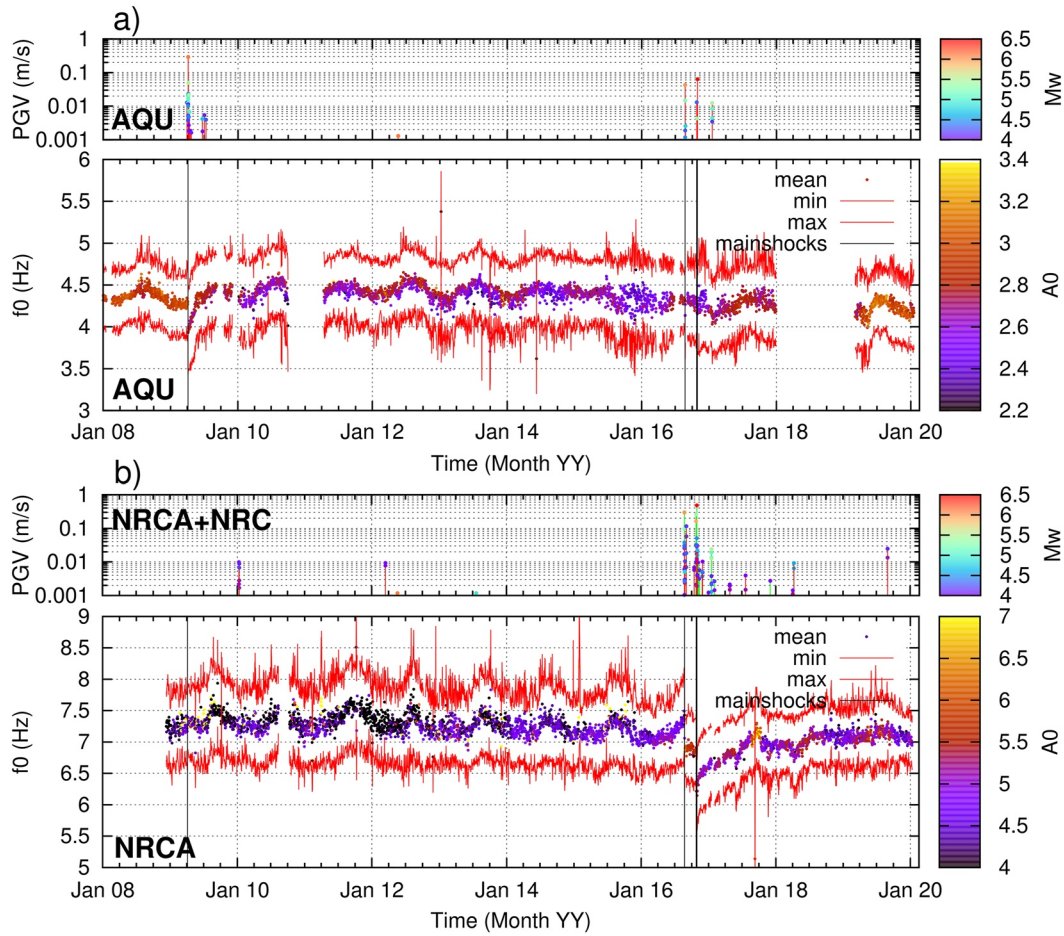

Figure 4. Temporal variation of the peak frequency ±1 standard deviation inferred from H/V on noise at the two stations: (a) AQU and (b) NRCA. Dots color is proportional to the H/V amplitude and black vertical lines indicate the time of the mainshocks occurrence (L'Aquila 06 April 2009, Mw 6.1; Amatrice 24 August 2016, Mw 6.0; Castelsantangelo sul Nera 26 October 2016, Mw 5.4; Visso 26 October 2016, Mw 5.9, and Norcia 30 October 2016, Mw 6.5). Upper plots for each station show the ground shaking in terms of PGV obtained by the integration of the accelerograms of the strong motion station. Note that there were no PGV values available (there was no accelerometric recording available for some of the main earthquakes) at NRCA (red vertical bars) for the largest shocks, for which we then used the PGV values of the closest accelerometric station NRC (green vertical bars). In the PGV plots, the color of points at the end of vertical bars represents the Mw magnitude associated with earthquakes.

The results of the coherence analysis between seismic H/V peak frequency and temperature are shown in Figure S4 in Supporting Information S1. In the following, we summarize the main results:

1. The variation with time of the peak frequency (f) is correlated with the one-year-period seasonal variation of temperature (T) but not with rainfall (P). In fact, the time series of f and T have a coherence larger than 0.7 around one-year period with a phase lag of frequency peak respect to temperature ranging from at least 10% of one-year cycle (40 days) for NRCA and 5% of one-year cycle (20 days) for AQU. Because the temperature variation is an indirect measure (proxy) of seasonal changes, we infer that the periodicity is clearly related to seasonality.
2. Although the weather stations are not colocated with the seismological ones, the time series smoothed with a 5-day window is able to catch the seasonal (one-year period) correlation with the frequency-peak variability in time. We cannot exclude correlation at smaller periods (days, weeks) that are probably more sensitive to the distance between weather and seismic stations.
3. The variability of the amplitude at the peak frequency (A) does not depend on temperature and rainfall variations. We observe only occasional correlation between the time series of A and temperature, or rainfall, at both stations.

4. There were no sudden changes (decreases) of temperature when mainshocks occurred (6 April 2009 for AQU; 24 August, 26 October, and 30 October 2016, for NRCA). Moreover, in the case of NRCA, the coherence decreases after the two mainshocks, whereas for AQU, the loss of correlation is less evident: the mainshock occurrence is at the edge of the cone of influence for the wavelet coherence (areas outside or overlapping the cone of influence are less reliable) and the frequency peak recovery is faster than for the NRCA case. These observations lead to the conclusion that the variations of the peak frequency after the earthquake occurrence do not depend on changes in temperature.

4. Spectral Ratio Analysis on Earthquakes

Because of the large availability of earthquakes during the analyzed period (Figure 1), the H/V ratios were also computed using only the earthquake signals. By using the bulletin of earthquake locations drawn up by the INGV surveillance service (http://terremoti.ingv.it/, last accessed in April 2022; ISIDe Working Group, 2007), we selected the events occurred at distances lower than 50 km from AQU and NRCA and with a local magnitude between 1.0 and 3.5. These criteria were adopted to have a good distribution and a large number of earthquakes over time, allowing us to estimate temporal variations of H/V ratios with a resolution comparable with the continuous data.

A total number of 15,211 earthquakes were processed for AQU (from 01 June 2008 to 17 January 2010) and 82,889 earthquakes for NRCA (from 24 August 2016 to 31 January 2020). Steps of processing were: (a) downloading the velocimetric waveforms (100 Hz sampling frequency) from EIDA (https://eida.ingv.it; last accessed in April 2022), (b) identification of the S-wave arrival at each station, (c) cutting a 6s long window starting from the theoretical S-waves arrival time, (d) selecting the records having the signal-to-noise ratio (SN) larger than 20, and (e) computing the H/V ratio by dividing the horizontal FAS by the vertical FAS. Similarly to the noise analysis, the horizontal FAS were joined using the squared average. Regarding the identification of S-wave arrival time, we estimated the theoretical travel time by means of the ray theory (*cake* software for travel-times and ray paths in 1D layered media, https://pyrocko.org/; Heimann et al., 2017), defining an S-wave velocity (V_s) monodimensional (1D) model for the investigated area that includes the epicenters of earthquakes and the analyzed station. This model is an average of the three-dimensional (3D) one computed from the tomographic inversion of regional seismic events (Di Stefano & Ciaccio, 2014, 2020). The automatic estimates of the S-wave arrival times are in good agreement with the real ones (Figure S5 in Supporting Information S1) and accurate enough for our aim, that is to individuate a 6-s-long time window containing the S waves.

The SN ratio is computed by dividing the peak velocity extracted in the 6-s-long window starting from the theoretical S arrival time with the root-mean-square (rms) average of a 6-s-long window before the P-wave arrival. We checked that this strategy for evaluating the SN ratio is more conservative than using the classical approach in the frequency domain, which is by dividing the Fourier spectra of signal and noise time windows. Moreover, adopting an SN threshold of 20 for accepting or disregarding the waveforms, we are sure to keep only the waveforms with a signal largely above the noise level.

Similar to the analysis on continuous data, the H/V ratio was computed using Geopsy in a batch mode for the 6-s-long windows after the S-wave arrival time (0.5–15 Hz frequency band and Konno-Ohmachi smoothing with $b = 40$). Then, the H/V results were averaged on 5-day intervals according to the origin time of the events. The results for the two stations are shown in the supplemental material (Figure S6 in Supporting Information S1). Starting from the main events and for a duration that depends on the triggered sequence (about 1.5 months in the case of L'Aquila and 1.5 years for the Central Italy sequence), in each 5-day interval, hundreds to thousands of events with different magnitude, distance, and azimuth respect to the station were averaged. With this criterion, we believe that the computation of the peak frequencies is very robust at least for the time windows in which many earthquakes occur.

The comparison of the peak frequencies computed on continuous data (red cross) and those computed using only the earthquakes (colored circles) is shown in Figure 5. For both stations, the agreement is good whether the H/V average on earthquakes comprises at least 100 events. This large number of events always occurs after the most energetic earthquakes, but there can be long "quiet" periods where few events of magnitude between 1 and 3.5 have been detected. The values of the peak frequencies obtained by averaging less than 100 events show a more

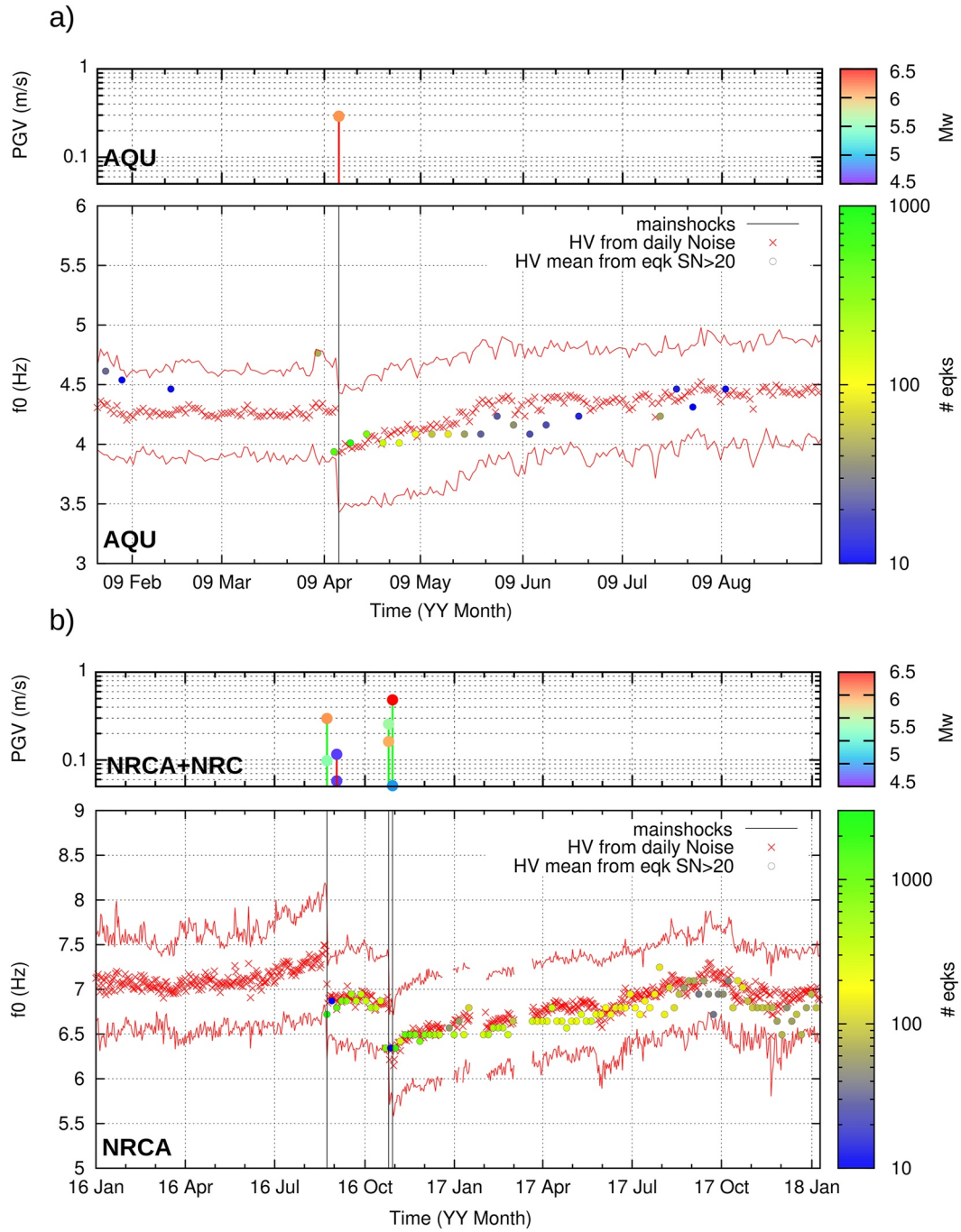

Figure 5. Temporal variation of peak frequencies from H/V on noise (red cross) and earthquakes (colored circles) at the two stations: (a) AQU and (b) NRCA. For each station, both the trend of the computed peak frequency (bottom panel) and the recorded PGV (higher than 0.05 m/s) are reported (top panel). In the panels showing the frequency variations, the red curves represent the uncertainty interval (±1 standard deviation) associated with the daily peak frequency calculated on the continuous recordings (red crosses). The circles show the 5-day average of the peak frequency obtained from the analysis of earthquakes. The color of the circles is linked to the number of earthquakes used for each 5-day interval. Finally, the black vertical lines indicate the time of the mainshock occurrences (L'Aquila 06 April 2009, Mw 6.1 for AQU station; Amatrice 24 August 2016, Mw 6.0, Visso 26 October 2016, Mw 5.9, and Norcia 30 October 2016, Mw 6.5 for NRCA station). In the panels showing the PGVs, the height of the vertical bars is proportional to the PGV values and the color of dots represent the magnitude of the corresponding earthquakes.

scattered trend over time and are generally lower (of about 0.2–0.3 Hz) than the corresponding peak frequencies obtained on the continuous data.

However, both noise and earthquakes show clear and impulsive drops in the peak frequency soon after the largest shocks (Figure 5). For AQU station, the peak frequency drops from 4.35 Hz to about 3.9 Hz at the occurrence of the 06 April 2009 L'Aquila earthquake (Figure 5a) and it recovers to the pre-event value in about 40 days. For NRCA, after the Mw 6.0 Amatrice event occurred on 24 August 2016 (Table 2), the peak frequency drops suddenly from 7.4 to 6.9 Hz (Figure 5b). The peak remains stable on this latter value until 26 October 2016 when two energetic earthquakes occurred (Castel Sant'Angelo sul Nera and Visso with Mw of 5.4 and 5.9, respectively, Chiaraluce et al., 2017; Improta et al., 2019). After them, the peak frequency decreases again, suddenly reaching the value of 6.2 Hz and then growing gently in the following year and a half until returning to the pre-event frequency value.

In Figure 5, the recorded PGV values are also plotted and used as a reference time mark of the occurrence of the strong events (Table 2). Unfortunately, for technical problems, there were no seismic records (Moretti et al., 2017) available at NRCA for some of the largest shocks. We then used the PGV values computed using the accelerograms of the trigger station NRC, belonging to the Italian Strong Motion Network run by the Italian Civil Protection Department (RAN; http://ran.protezionecivile.it), and located about 5 km southwest of the NRCA station (Table1). By comparing the variability of the peak frequencies with the PGV values at AQU and NRCA, it can be inferred that the peak frequency for both sites shows a sharp decrease whenever a strong motion occurs. In terms of PGV, peak frequency variations are observed when PGV is larger than about 0.2 m/s (Table 2 and Figure 5). This is the case of the 6 April 2019, L'Aquila earthquake at AQU (Figure 4a) and the 2016 mainshocks (Amatrice and Castelsantangelo-Visso earthquakes) at NRCA (Figure 5b).

Comparing the available PGV values (Figure S7 in Supporting Information S1), NRC recorded lower PGV than NRCA during several strong events of the Central Italy sequence. It is therefore plausible that when the frequency shift occurred at NRCA, the PGV value at this station was probably greater than 0.2 m/s.

It is important to underline that not all earthquakes producing shaking greater than 0.2 m/s generated a drop in peak frequency. This is evident by a detailed analysis of the peak frequency variations and measured PGVs at NRCA and NRC stations (Figure 5) during the 2016 Central Italy sequence. The most energetic event that occurred in the Central Italy seismic sequence, the Norcia earthquake of 30 October 2016 (Mw 6.5; Table 2), seems not to significantly affect the peak frequency even though it has generated significant ground shaking with PGV equal to 0.48 m/s. This could be explained observing that several important earthquakes had occurred in the same area just few days before (24 August 2016 Amatrice, Mw 6.0; 26 October 2016 Castelsantangelo sul Nera, Mw 5.4, and 26 October 2016 Visso, Mw 5.9) causing ground shaking with PGV higher than 0.2 m/s and peak frequency drop. In particular, the Castelsantangelo sul Nera and the Visso events occurred just 4 days before the Norcia earthquake.

5. Discussion

Spectral ratios at AQU and NRCA stations, carried out on 12 years of continuous data, highlight clear temporal variations of the H/V peak frequencies. They can be of two different types: seasonal and impulsive after strong shakings. The first variation is cyclical with a period of one year within ± 2%–3% around the yearly average and is likely linked to seasonal changes: we observe an increase in frequency during the spring/summer seasons and a decrease in autumn/winter. By matching the obtained frequencies perturbation with the available weather data near the stations, we observed a good correlation (coherence factor >0.7) with the averaged air temperature (a parameter that we used as a proxy to characterize the seasonality of the sites). This result is in good agreement with Colombero et al. (2018) that finds a direct linear correlation between H/V peak frequency and air temperature from noise measurements acquired at a potentially unstable cliff of Madonna del Sasso (NW Italian Alps). Moreover, the phase lag of frequency peak with respect to the temperature at the maximum coherence (i.e., around one-year-period) is almost stable over the investigated years and has a delay of at least 40 days for NRCA and 20 days for AQU. The delay difference between the 2 stations indicates that it is more likely related to the changes in the soil itself (e.g., changing water level, etc.) rather than on large-scale effects, such as the moving of the microseismic noise source over the year whose effects are expected to manifest almost simultaneously at the two stations.

The second type of variation is characterized by a sudden decrease in the peak frequencies when moderate-to-strong earthquakes occur near the stations. For both stations, these variations have a sharp frequency decrease in the H/V peak after each mainshock, followed by a gradual recovery to the pre-event value in a time that varies from more than a month to a few years (Figure 4). In particular, AQU experienced a reduction of the mean frequency peak from 4.35 to 3.9 Hz for the 2009 L'Aquila earthquake, which corresponds to a 10% drop. Whereas NRCA peak decreased from 7.4 to 6.9 Hz for the 2016, 24th August, Amatrice earthquake (7% drop) and from 6.9 to 6.2 Hz (10% drop) for the 26th October Visso earthquake (Figure 4).

Variations in resonance frequencies following particularly energetic earthquakes in the world (Duzce 12 December 1999 Mw 7.2; Western Tottori 06 October 2000, Mw 6.7; Tokachi-Oki 25 September 2003, Mw 8.3; Tohoku 03 November 2011, Mw 9.0) have been already observed by several authors by using spectral ratios. The ratios are computed in different ways: from earthquake horizontal spectra for the surface and borehole stations (Sawazaki et al., 2006; Wu & Peng, 2011, 2012), from spectral ratios of strong motion recorded by pairs of non-collocated stations (Wu et al., 2009), and from autocorrelation in moving time window of earthquake waveforms (Bonilla et al., 2019, 2021). Sawazaki et al. (2006), after the Mw 6.7 Western Tottori and Mw 8.3 Tokachi-Oki earthquakes, observed a reduction of the peak frequency of 30%–70% followed by a frequency recovery variable from a few tens of minutes up to a few years. Wu and Peng (2012) found a clear drop of the resonant frequency of up to 70% during the Mw 9.0 Tohoku main shock, followed by a rapid post-seismic recovery in the first few hundred seconds to several hours and then a much longer-term slow recovery of at least 5 months. Wu et al. (2009) found that during the 1999 Duzce earthquake, the peak frequency in the fault zone dropped ∼20%–40% and recovered with a time scale of ∼1 day (they were not able to determine whether long-term recovery exists or not after 1 day). Bonilla et al. (2021) observed resonance frequency changes of about 10% at the occurrence of Mw 9.0 Tohoku earthquake with a full recovery in 20–90 days depending on the frequency: slower in the range 3–10 Hz and faster for higher frequencies. This evidence prompts the authors to suggest a depth dependency of the perturbation after a large event with the shallower layers, which recovers faster than the deeper layers. In the present work, we observe a different behavior with longer recovery time for NRCA (frequency peak of 7.3 Hz) than for AQU (frequency peak of 4.3 Hz). According to Wu and Peng (2012), the recovery time to the initial state before a strong earthquake depends on site conditions, input ground motion, and other minor factors. For AQU and NRCA, the recoveries may strongly depend on the very different evolution of the two seismic sequences as well as the different seismic and rheological behavior at the two sites. Moreover, the different amount of frequency shift can play a role in the recovery. NRCA has experienced a larger number of strong motions, two of which produced a cumulative peak frequency variation equal to 16% (from 7.4 Hz before the first mainshock to 6.2 Hz after the second one), whereas AQU was hit only by the mainshock Mw 6.1 that produced a unique peak frequency drop with a reduction equal to 10%.

Sawazaki et al. (2006, 2009) and Hobiger et al. (2016) observed a logarithmic recovery trend lasting a few years and several years (with only partial recovery over the observation time), respectively. Differently from the above-mentioned papers, in the present study, the analysis was carried out on the H/V spectral ratios from single stations computed on the continuous velocimetric data and on small magnitude (M_L 1–3.5) events. The H/V method, based on the availability of many years of recordings, allowed us to follow the slow recovery phase with a good temporal continuity. The use of continuous data and/or small-magnitude events offers the advantage of assessing peak frequency variations regardless of the abundance of strong earthquakes in the recorded seismic sequence and it can be applied also at the occurrence of moderate-magnitude earthquakes.

Under the diffuse field assumption (Sanchez-Sesma et al., 2011), H/V is interpreted as related to the imaginary part of the Green's Function when both source and receiver are located at the same place. Interferometric methods are used to extract the Green's Functions through the computation of autocorrelation functions at a single station or cross-correlation functions at station pairs using the seismic noise. Interferometric methods are effective for monitoring changes of the seismic-wave velocity because the continuous Green's functions can track time changes in physical parameters of the crust. Considering the link between Green's functions and the H/V ratios, it is reasonable to expect that seismic velocity changes of the propagation medium can affect, in some way, the H/V functions.

Nonlinearity of the soils is generally invoked to interpret the temporal changes of seismic velocities after the occurrence of strong earthquakes. In these cases, the main observed effect is the shift of the resonance frequency (Bonilla et al., 2019; Pei et al., 2019). Velocity variations are connected to:

1. Opening (and closing) of cracks induced by changes of the stress field that causes decrease (and increase) of the seismic velocities of propagation media
2. Structural changes within the rupture zone associated with the subsurface stress field (due to coseismic damaging and subsequent postseismic healing, earthquake nucleation, and other preseismic phenomena)
3. Changes in the fluid content at different depths and liquefaction behavior at shallow layers.

The first two points are generally related to crustal wavelengths and are invoked in seismic noise studies for phenomena occurring at low frequencies (below 0.5–1 Hz). The third point is more suitable for explaining the velocity variation in shallower sedimentary soils in connection with matrix damages and pore pressures effects. Considering the frequencies involved in this work (greater than 1 Hz), this interpretation could better explain the observed variations in peak frequencies.

Although in this paper we focus on the H/V technique, the Vs changes are commonly studied with interferometric techniques based on seismic noise cross correlations (Brenguier et al., 2008; Cheng et al., 2010; Wegler and Sens-Schonfelder, 2007). The same techniques are also used in experiments performed in underground mines to examine the influence of dynamic and static stress perturbations on seismic velocities (Olivier et al., 2015). These studies show a quick drop of V_s after the occurrence of a strong earthquake, followed by a slow relaxation that restores the velocities back to preseismic levels. The instantaneous weakening and the gradual healing are a very similar behavior if compared to what we observe for the H/V peak frequencies at AQU and NRCA.

The frequencies of H/V peaks are, in the first approximation, directly proportional to the Vs properties of resonant layers, then it is reasonable to hypothesize that the observed variations are associated with velocity changes of the near-surface model below the station. Under this hypothesis, it is possible to roughly estimate the V_s changes from the 1D relation $V_s = f/4h$ that links the peak frequency (f), the velocity (V_s), and the thickness of the layer (h). This latter parameter is supposed to be constant. As a first approximation, the percentage of V_s variation in the surface layers corresponds to the peak frequency reduction observed at the stations (Bonilla & Ben-Zion, 2021), for example, 10% for AQU ($f = 4.3$ Hz) and 7%–10% for NRCA ($f = 7.3$ Hz), respectively. Note that for AQU station, the lowest resonant frequency (at 0.55 Hz) does not show significant changes when the earthquake occurs, probably because the effect of the shallow layer is too small to be appreciated on such a low peak frequency. Considering the frequencies involved in the drop effect observed for AQU and NRCA, the cross correlations computed on distant station pairs are generally unable to provide a measure of the velocity changes, which could instead be extracted from interferometric analyses by nearby stations or by the autocorrelation using noise acquired at single stations. Indeed, studies based on the autocorrelation functions computed from single-station noise data, find velocity changes of the order of a few percent in the frequency band of 2–5 Hz (Minato et al., 2012) and 1–3 Hz (Yukutake et al., 2016). Moreover, some of these studies suggest that the shallower layer experienced larger velocity reductions than the deeper subsurface (Hobiger et al., 2012, 2014; Minato et al., 2012). These interferometric studies are based on the assumption that results are mainly related to surface waves. The similarity between our results and the interferometric ones leads us to hypothesize that the surface waves have a dominant role in the determination of the observed velocity variations.

Velocity changes of a similar extent to our study were observed in Japan after the 2011 Tohoku-Oki earthquake by deconvolving waveforms recorded by Japanese stations at the surface and in a borehole (Nakata & Snieder, 2011): the authors detected a reduction of shear-wave velocity in the upper 100 m up to about 10% and retrieved a mean Vs reduction of about 5% for an area in northeastern Japan about 1,200 km wide.

In our study, the peak frequency drops occurred when strong shaking has affected the measurement sites. Unfortunately, we have only a few observations regarding the influence of the shaking intensity in the peak frequency (and velocity) variation to be able to extrapolate a general rule about this type of correlation. Furthermore, we observed that a strong shaking higher than a threshold of 0.2 m/s is not always sufficient to trigger a peak frequency drop. The best example is the strongest event of the Centro Italia sequence (30 October 2016 Norcia earthquake) well above the threshold but not producing the frequency drop at NRCA. This effect could be related to the cumulative effect of frequency drop after the occurrence of two other significant earthquakes that preceded the most energetic seismic event by 2 months and a few days, respectively. These observations are in agreement with the remarks made by Hobiger et al. (2016), which by performing a systematic study of seismic velocity changes associated with a megathrust and five strong crustal earthquakes in Japan, reach the conclusion that the

PGV values certainly play an important role in the explanation of the coseismic velocity changes, but they cannot fully explain the coseismic velocity changes.

6. Conclusion

Significant temporal variations of H/V spectral ratios have been detected by a massive analysis of 12 years of continuous data acquired by two permanent seismic stations operating in the Central Apennines (Italy). Our study highlighted two main time peak-frequency variations observed at both stations. The peak frequency is affected by temporal variations related to the alternation of seasonal cycles and a quick decrease at the occurrence of strong earthquakes located near the sites. The ways in which the peak-frequency changes over time and the close analogy between the H/V spectral ratios with the Green's Functions allow us to interpret the result in terms of reductions of the velocity V_s of the shallow layers. In the reasonable assumption that the strong earthquakes do not alter the thickness of the layers, the resonant frequency perturbation can be entirely translated into V_s decrease in the layers. V_s reductions obtained in this work are therefore of the same order of peak frequency variations, which are about 7%–10%. These estimates must be interpreted as the average change of shear-wave velocity above the impedance contrast generating the H/V frequency peak. We expect that the velocity variation is higher in the shallower and softer sublayers, but we do not have the necessary resolution in the seismic/rheological model to investigate the contribution of a single sublayer in the observed frequency shift. Due to this lack of information on both sites, we are not able to exactly identify where the velocity changes take place and why the frequency recovery time observed at the two sites is different. Moreover, it is worth noting that the V_{s30} is relatively high at both AQU and NRCA sites, but being an average velocity, it can hide the presence of very thin soft layers that can be in principle responsible for the observed effects.

Taking into account the role of the frequency ranges used in estimating velocity variations, our observations are in good agreement with variations obtained from interferometric studies. Indeed, velocity reductions of the same order of magnitude to those obtained in this work are observed by autocorrelation analysis (Minato et al., 2012; Yukutake et al., 2016) and by interferometric analysis performed to study velocity variations in the upper few hundred meters after the Tohoku-Oki earthquake (Nakata & Snieder, 2011). Unlike the interferometric analysis based on seismic noise, where the variations are usually averaged over few tens of days up to some months, the H/V spectral ratio analyses carried out on long portions of the signal (months and years) provide the evolution of peak frequencies, and related shear-wave velocities, on much narrower time scales. The temporal resolution is connected to the length of the time windows used to average the H/V estimates that in this work is equal to 1 day and 5 days for results obtained using noise and earthquake data, respectively.

The study described in this paper demonstrates that the H/V analysis performed on continuously recorded noise and/or on small magnitude events is a tool able to provide important information on temporal velocity variations involving the shallow layers. In the case of strong earthquakes, such information is typically obtained through a spectral ratio of horizontal components and/or interferometric analyses on individual strong-motion records. Compared to these methods, the computation of the H/V spectral ratio over time as carried out in this work allows us to estimate the variations of the peak frequency and seismic velocities with a lower temporal resolution, not sufficient to retrieve the resonant frequency variations associated with mainshocks (coseismic variations). However, the H/V analysis over time provides the frequency variation with temporal continuity regardless of the occurrence of strong earthquakes in the recorded seismic sequence, allowing the reconstruction of the frequency recovery phase also in cases which is temporally very long. In addition, the proposed analysis method can be applied also at the occurrence of moderate-magnitude earthquakes, since it requires just continuous seismic recordings. In the future, it will be necessary to investigate the possibility of reducing the time windows used to average the H/V estimates. This could provide results with an improved temporal resolution, providing the opportunity for detection of the rapid peak frequency recovery stage (Wu & Peng, 2012).

The present study shows the importance of applying the spectral ratio analysis on years-long time series. The availability of continuous data from permanent seismic networks allows the implementation of our analysis to other stations close to seismic areas both in Central Italian Apennines and in other sites with different soil characteristics. In this way, it will be possible to bring out the temporal spectral relationships due to seasonal and to moderate/strong earthquake-induced variations of the ground geophysical properties of the shallow layers together with a detailed analysis on whether higher frequencies heal faster or slower than lower frequencies.

The velocity variations extracted from the temporal variations of H/V can be attributed to very shallow layers (from a few tens up to a few hundred meters). This information is very important for engineering and microzonation applications. For example, very often, the evaluations of the fundamental frequencies for microzonation studies are carried out in epicentral areas immediately after the occurrence of strong earthquakes. Based on the results produced in this work, these studies could underestimate the main peak frequencies that characterize the measurement sites.

Moreover, it will be important to study the possible role of variations in groundwater levels in the peak frequency changes observed by the long-term H/V analysis. Several authors (Berbellini et al., 2021; Clements & Denolle, 2018; Poli et al., 2020) have shown that it is possible to follow groundwater level changes by performing the interferometric analysis for the determination of seismic velocity versus time. The analysis based on the H/V spectral ratio could provide interesting information on the groundwater processes (as multiyear depletions and rapid recharges of aquifers), especially when the depth to the water table is very shallow. For an established site of interest, the comparison between the results produced by H/V with those deduced from interferometric techniques and from crustal deformation data measured with the Global Positioning System (GPS) may highlight the potential of the methodology proposed in this work in the monitoring of groundwater storage.

Data Availability Statement

The two stations (AQU and NRCA) belong to Italian permanent network (hereinafter RSN; INGV Seismological Data Centre, 2006; Margheriti et al., 2021) operated by the Istituto Nazionale di Geofisica e Vulcanologia (INGV). Their data were downloaded from the European Integrated Data Archive (EIDA, https://eida.ingv.it last accessed in April 2022; Strollo et al., 2021). Geophysical and geological information for NRCA and AQU can be downloaded from the INGV database for the site characterization of the permanent seismic stations (http://crisp.ingv.it; https://doi.org/10.13127/crisp). Rain and temperature data of L'AQUILA meteorological station are provided under request to the Territory–Environment Department of the Abruzzo region (Civil Protection Activities Planning Service, Hydrographic and Oceanographic Office), through a form on their website (https://www.regione.abruzzo.it/content/servizio-idrografico-mareografico); data up to 2011 only are freely available on https://www.regione.abruzzo.it/content/annali-idrologici. Data of NORCIA meteorological station are provided by the Hydrographic Service of Umbria region (https://servizioidrografico.regione.umbria.it) and can be downloaded from a dedicated website (https://annali.regione.umbria.it/; https://servizioidrografico.regione.umbria.it/pdf_stazioni/0000201100_Norcia.pdf). The data at both meteorological stations are raw and the providers are relieved of all responsibility for the use of the data provided.

Acknowledgments

We thank the editor, the associated editor, and the two reviewers, Fabian Bonilla and Manuel Hobiger, for their constructive and interesting comments that largely improved the paper. This study has benefited from funding provided by the Italian Presidenza del Consiglio dei Ministri—Dipartimento della Protezione Civile (DPC). This paper does not necessarily represent DPC official opinion and policies. Open Access Funding provided by Istituto Nazionale di Geofisica e Vulcanologia within the CRUI–CARE Agreement.

References

Albarello, D., Cesi, C., Eulilli, V., Guerrini, F., Lunedei, E., Paolucci, E., et al. (2011). The contribution of the ambient vibration prospecting in seismic microzoning: An examBollettino di Geofisica Teorica ed Applicataple from the area damaged by the April 6, 2009 L'aquila (Italy) earthquake. *Bollettino di Geofisica Teorica ed Applicataple*, *52*, 513–538.

Amanti, M., Muraro, C., Roma, M., Chiessi, V., Puzzilli, L. M., Catalano, S., et al. (2020). Geological and geotechnical models definition for 3rd level seismic microzonation studies in Central Italy. *Bulletin of Earthquake Engineering*, *18*(12), 5441–5473. https://doi.org/10.1007/s10518-020-00843-x

Arai, H., & Tokimatsu, K. (2004). S-wave velocity profiling by inversion of microtremor H/V spectrum. *Bulletin of the Seismological Society of America*, *94*(1), 53–63. https://doi.org/10.1785/0120030028

Berbellini, A., Zaccarelli, L., Faenza, L., Garcia, A., Improta, L., De Gori, P., & Morelli, A. (2021). Effect of groundwater on noise-based monitoring of crustal velocity changes near a produced water injection well in val d'Agri (Italy). *Frontiers of Earth Science*, *9*, 197. https://doi.org/10.3389/feart.2021.626720

Bonilla, L. F., & Ben-Zion, Y. (2021). Detailed space–time variations of the seismic response of the shallow crust to small earthquakes from analysis of dense array data. *Geophysical Journal International*, *225*(1), 298–310. https://doi.org/10.1093/gji/ggaa544

Bonilla, L. F., Guéguen, P., & Ben-Zion, Y. (2019). Monitoring coseismic temporal changes of shallow material during strong ground motion with interferometry and autocorrelation. *Bulletin of the Seismological Society of America*, *109*(1), 187–198. https://doi.org/10.1785/0120180092

Bonilla, L. F., Guéguen, P., & Gélis, C. (2021). Contribution of KNET and KIK-NET data to the monitoring of nonlinear properties of shallow crust. In *ESC6 - 6th IASPEI/IAEE international symposium: Effects of surface geology on seismic motion*.

Bordoni, P., Del Monaco, F., Milana, G., Tallini, M., & Haines, J. (2014). The seismic response at high frequency in central L'Aquila: A comparison between spectral ratios of 2D modeling and observations of the 2009 aftershocks. *Bulletin of the Seismological Society of America*, *104*(3), 1374–1388. https://doi.org/10.1785/0120130230

Bormann, P., & Wielandt, E. (2013). Seismic signals and noise. In P Bormann(Ed.), *New manual of seismological observatory practice 2 (NMSOP2), potsdam: Deutsches GeoForschungsZentrum GFZ* (pp. 1–62). https://doi.org/10.2312/GFZ.NMSOP-2_ch4

Bour, M., Fouissac, D., Dominique, P., & Martin, C. (1998). On the use of microtremor recordings in seismic microzonation. *Soil Dynamics and Earthquake Engineering*, *17*(7–8), 465–474. https://doi.org/10.1016/s0267-7261(98)00014-1. ISSN 0267-7261

Brandonisio, G., Lucibello, G., Mele, E., & De Luca, A. (2013). Damage and performance evaluation of masonry churches in the 2009 L'Aquila earthquake. *Engineering Failure Analysis*, *34*, 693–714. https://doi.org/10.1016/j.engfailanal.2013.01.021

Brenguier, F., Campillo, M., Hadziioannou, C., Shapiro, N. M., Nadeau, R. M., & LaRose, E. (2008). Postseismic relaxation along the San Andreas fault at parkfield from continuous seismological observations. *Science*, *321*(5895), 1478–1481. https://doi.org/10.1126/science.1160943

Cen. (2004). *Eurocode (EC) 8. Design of structures for earthquake resistance – Part 1 General rules, seismic actions and rules for buildings (EN 1998-1)*.

Cheng, X., Niu, F., & Wang, B. S. (2010). Coseismic velocity change in the rupture zone of the 2008 Mw 7.9 Wenchuan Earthquake observed from ambient seismic noise. *Bulletin of the Seismological Society of America*, *100*(5B), 2539–2550. https://doi.org/10.1785/0120090329

Chiaraluce, L., Chiarabba, C., De Gori, P., Di Stefano, R., Improta, L., Piccinini, D., et al. (2010). *The 2009 L'Aquila (Central Italy) Seismic Sequence. Bollettino di Geofisica Teorica e Applicata*.

Chiaraluce, L., Di Stefano, R., Tinti, E., Scognamiglio, L., Michele, M., Casarotti, E., et al. (2017). The 2016 central Italy seismic sequence: A first look at the mainshocks, aftershocks, and source models. *Seismological Research Letters*, *88*(3), 757–771. https://doi.org/10.1785/0220160221

Cirella, A., Piatanesi, A., Tinti, E., Chini, M., & Cocco, M. (2012). Complexity of the rupture process during the 2009 L'Aquila, Italy, earthquake. *Geophysical Journal International*, *190*(1), 607–621. https://doi.org/10.1111/j.1365-246x.2012.05505.x

Civico, R., Pucci, S., Villani, F., Pizzimenti, L., De Martini, P. M., & Nappi, R., & Open EMERGEO Working Group. (2018). Surface ruptures following the 30 October 2016 Mw 6.5 Norcia earthquake, central Italy. *Journal of Maps*, *14*(2), 151–160. https://doi.org/10.1080/17445647.2018.1441756

Clements, T., & Denolle, M. A. (2018). Tracking groundwater levels using the ambient seismic field. *Geophysical Research Letters*, *45*(13), 6459–6465. https://doi.org/10.1029/2018GL077706

Colombero, C., Baillet, L., Comina, C., Jongmans, D., Larose, E., Valentin, J., & Vinciguerra, S. (2018). Integration of ambient seismic noise monitoring, displacement and meteorological measurements to infer the temperature-controlled long-term evolution of a complex prone-to-fall cliff. *Geophysical Journal International*, *213*(3), 1876–1897. https://doi.org/10.1093/gji/ggy090

Cultrera, G., Bordoni, P., Casale, P., Cara, F., Di Giulio, G., Famiani, D., et al. (2018). Site characterization database of INGV Italian seismic network. S34 - developments in strong motion seismology, a COSMOS session. ESC-S34-872. *The European seismological commission ESC2018 36th general assembly, 2–7 sept. 2018*. La Valletta.

Cultrera, G., Cornou, C., Di Giulio, G., & Bard, P.-Y. (2021). Indicators for site characterization at seismic station: Recommendation from a dedicated survey. *Bulletin of Earthquake Engineering*, *19*(11), 4171–4195. https://doi.org/10.1007/s10518-021-01136-7

Cultrera, G., De Rubeis, V., Theodoulidis, N., Cadet, H., & Bard, P. Y. (2014). Statistical correlation of earthquake and ambient noise spectral ratios. *Bulletin of Earthquake Engineering*, *12*(4), 1493–1514. https://doi.org/10.1007/s10518-013-9576-7

D'Amico, M., Felicetta, C., Russo, E., Sgobba, S., Lanzano, G., Pacor, F., & Luzi, L. (2020). *Italian Accelerometric Archive v 3.1 - Istituto Nazionale di Geofisica e Vulcanologia, Dipartimento della Protezione Civile Nazionale*. https://doi.org/10.13127/itaca.3.1

Di Stefano, R., & Ciaccio, M. G. (2014). The lithosphere and asthenosphere system in Italy as inferred from the Vp and vs 3D velocity model and Moho map. *Journal of Geodynamics*, *82*, 16–25. https://doi.org/10.1016/j.jog.2014.09.006

Di Stefano, R., & Ciaccio, M. G. (2020). Seismic velocity model of P- and S-waves for the Italian lithosphere (1.0). [Data set]. https://doi.org/10.13127/tomorama.1

Endrun, B. (2011). Love wave contribution to the ambient vibration H/V amplitude peak observed with array measurements. *Journal of Seismology*, *15*(3), 443–472. https://doi.org/10.1007/s10950-010-9191-x

Fäh, D., Kind, F., & Giardini, D. (2001). A theoretical investigation of average H/V ratios. *Geophysical Journal International*, *145*(2), 535–549. https://doi.org/10.1046/j.0956-540x.2001.01406.x

Felicetta, C., Mascandola, C., Spallarossa, D., Pacor, F., Hailemikael, S., & Di Giulio, G. (2021). Quantification of site effects in the Amatrice area (Central Italy): Insights from ground-motion recordings of the 2016–2017 seismic sequence. *Soil Dynamics and Earthquake Engineering*, *142*, 106565. https://doi.org/10.1016/j.soildyn.2020.106565

Field, E. H., & Jacob, K. H. (1995). A comparison and test of various site-response estimation techniques, including three that are not reference-site dependent. *Bulletin of the Seismological Society of America*, *85*(4), 1127–1143.

Galli, P. & Camassi, R. (Eds.). (2009). *Rapporto sugli effetti del terremoto aquilano del 6 aprile 2009, DPC-INGV QUEST Team*. Retrieved From http://www.mi.ingv.it/eq/090406/quest.html

Galli, P., Castenetto, S., & Peronace, E. (2017). The macroseismic intensity distribution of the 30 October 2016 earthquake in central Italy (Mw 6.6): Seismotectonic implications. *Tectonics*, *36*(10), 2179–2191. https://doi.org/10.1002/2017tc004583

Garcıa-Jerez, A., Luzon, F., Albarello, D., Lunedei, E., Sanchez-Sesma, F. J., & Santoyo, M. A. (2012). Comparison between ambient vibration H/V synthetics obtained from the diffuse field approach and from the distributed surface load method. In *Proceedings of the XXIII general assembly of the European seismological commission* (pp. 412–413). (ESC 2012), 25–30 Aug 2012.

Garcıa-Jerez, A., Luzon, F., Sanchez-Sesma, F. J., Santoyo, M. A., Albarello, D., Lunedei, E., et al. (2011). Comparison between two methods for forward calculation of ambient noise H/V spectral ratios. *AGU fall meeting* (pp. S23A–2230). Retrieved from http://abstractsearch.agu.org/meetings/2011/FM/sections/S/sessions/S23A/abstracts/S23A-2230.html

GEER-050D Report. (2017). *Engineering Reconnaissance following the October 2016 Central Italy Earthquakes, version 2*, In P. Zimmaro & J. P. Stewart (Eds.), GEER Team Leaders, J. P. Stewart, & G. Lanzo. https://doi.org/10.18118/G6HS39

Haghshenas, E., Bard, P. Y., Theodulidis, N., & SESAME WP04 Team. (2008). Empirical evaluation of microtremor H/V spectral ratio. *Bulletin of Earthquake Engineering*, *6*(1), 75–108. https://doi.org/10.1007/s10518-007-9058-x

Heimann, S., Kriegerowski, M., Isken, M., Cesca, S., Daout, S., Grigoli, F., et al. (2017). *Pyrocko - an open-source seismology toolbox and library*. V. 0.3. GFZ Data Services. https://doi.org/10.5880/GFZ.2.1.2017.001

Herak, M. (2008). ModelHVSR: A Matlab® tool to model horizontal-to-vertical spectral ratio of ambient noise. *Computers & Geosciences*, *34*(11), 1514–1526. https://doi.org/10.1016/j.cageo.2007.07.009

Hobiger, M., Wegler, U., Shiomi, K., & Nakahara, H. (2012). Coseismic and postseismic elastic wave velocity variations caused by the 2008 Iwate-Miyagi Nairiku earthquake, Japan. *Journal of Geophysical Research*, *117*(B9), B09313. https://doi.org/10.1029/2012JB009402

Hobiger, M., Wegler, U., Shiomi, K., & Nakahara, H. (2014). Single-station cross-correlation analysis of ambient seismic noise: Application to stations in the surroundings of the 2008 iwate-miyagi nairiku earthquake. *Geophysical Journal International*, *198*(1), 90–109. https://doi.org/10.1093/gji/ggu115

Hobiger, M., Wegler, U., Shiomi, K., & Nakahara, H. (2016). Coseismic and post-seismic velocity changes detected by passive image interferometry: Comparison of one great and five strong earthquakes in Japan. *Geophysical Journal International*, *205*(2), 1053–1073. https://doi.org/10.1093/gji/ggw066

Hunter, J. A., & Crow, H. L. (Eds.), (2012). Shear wave velocity measurement guidelines for Canadian seismic site characterization in soil and rock. Geological Survey of Canada, Open File 7078, 227. https://doi.org/10.4095/291753

Improta, L., Latorre, D., Margheriti, L., Nardi, A., Marchetti, A., Lombardi, A. M., et al. (2019). The Bollettino Sismico Italiano Working Group. Multi-segment rupture of the 2016 Amatrice-Visso-Norcia seismic sequence (central Italy) constrained by the first high-quality catalog of Early Aftershocks. *Scientific Reports*, *9*(1), 6921. https://doi.org/10.1038/s41598-019-43393-2

INGV Seismological Data Centre. (2006). *Rete Sismica Nazionale (RSN), Istituto Nazionale di Geofisica e Vulcanologia (INGV), Italy*. https://doi.org/10.13127/SD/X0FXNH7QFY

ISIDe Working Group. (2007). *Italian Seismological Instrumental and Parametric Database (ISIDe), Istituto Nazionale di Geofisica e Vulcanologia (INGV)*. https://doi.org/10.13127/ISIDE

Köhler, A., & Weidle, C. (2019). Potentials and pitfalls of permafrost active layer monitoring using the HVSR method: A case study in svalbard. *Earth Surface Dynamics*, *7*, 1–16. https://doi.org/10.5194/esurf-7-1-2019

Konno, K., & Ohmachi, T. (1998). Ground-motion characteristics estimated from spectral ratio between horizontal and vertical components of microtremor. *Bulletin of the Seismological Society of America*, *88*(1), 228–241. https://doi.org/10.1785/bssa0880010228

Kula, D., Olszewska, D., Dobiński, W., & Glazer, M. (2018). Horizontal-to-vertical spectral ratio variability in the presence of permafrost. *Geophysical Journal International*, *214*(1), 219–231. https://doi.org/10.1093/gji/ggy118

La Rocca, M., Chiappetta, G. D., Gervasi, A., & Festa, R. L. (2020). Non-stability of the noise HVSR at sites near or on topographic heights. *Geophysical Journal International*, *222*(3), 2162–2171. https://doi.org/10.1093/gji/ggaa297

Lontsi, A. M., Sánchez-Sesma, F. J., Molina-Villegas, J. C., Ohrnberger, M., & Krüger, F. (2015). Full microtremor H/V (z, f) inversion for shallow subsurface characterization. *Geophysical Journal International*, *202*(1), 298–312. https://doi.org/10.1093/gji/ggv132

Lotti, A., Pazzi, V., Saccorotti, G., Fiaschi, A., Matassoni, L., & Gigli, G. (2018). HVSR analysis of rockslide seismic signals to assess the subsoil conditions and the site seismic response. *International Journal of Geophysics*. https://doi.org/10.1155/2018/9383189

Lunedei, E., & Albarello, D. (2010). Theoretical HVSR curves from full wavefield modelling of ambient vibrations in a weakly dissipative layered Earth. *Geophysical Journal International*, *181*(2), 1093–1108.

Lunedei, E., & Malischewsky, P. (2015). A review and some new issues on the theory of the H/V technique for ambient vibrations. In A. Ansal (Ed.), *Perspectives on European earthquake engineering and seismology*. *Geotechnical, geological and earthquake engineering* (Vol. 39). Springer.

Luzi, L., Hailemikael, S., Bindi, D., Pacor, F., Mele, F., & Sabetta, F. (2008). ITACA (Italian ACcelerometric archive): A web portal for the dissemination of Italian strong-motion data. *Seismological Research Letters*, *79*(5), 716–722. https://doi.org/10.1785/gssrl.79.5.716

Luzi, L., Puglia, R., Russo, E., & ORFEUS, WG5. (2016). Engineering strong motion database, version 1.0. *Istituto Nazionale di Geofisica e Vulcanologia, Observatories & Research Facilities for European Seismology*. https://doi.org/10.13127/ESM

Macerola, L., Tallini, M., Di Giulio, G., Nocentini, M., & Milana, G. (2019). The 1-D and 2-D seismic modeling of deep quaternary basin (downtown L'aquila, central Italy). *Earthquake Spectra*, *35*(4), 1689–1710. https://doi.org/10.1193/062618EQS166M

Margheriti, L., Nostro, C., Cocina, O., Castellano, M., Moretti, M., Lauciani, V., et al. (2021). Seismic surveillance and earthquake monitoring in Italy. *Seismological Research Letters*, *92*(3), 1659–1671. https://doi.org/10.1785/0220200380

McNamara, D. E., & Buland, R. P. (2004). Ambient noise levels in the con-tinental United States. *Bulletin of the Seismological Society of America*, *94*(4), 1517–1527. https://doi.org/10.1785/012003001

MedNet Project Partner Institutions. (1990). Mediterranean very broadband seismographic network (MedNet). *Istituto Nazionale di Geofisica e Vulcanologia (INGV)*. https://doi.org/10.13127/SD/FBBBTDTD6Q

Megies, T., Beyreuther, M., Barsch, R., Krischer, L., & Wassermann, J. (2011). ObsPy – what can it do for data centers and observatories? *Annals of Geophysics*. Retrieved From https://www.annalsofgeophysics.eu/index.php/annals/article/view/4838

Milana, G., Azzara, R. M., Bertrand, E., Bordoni, P., Cara, F., Cogliano, R., et al. (2011). The contribution of seismic data in microzonation studies for downtown L'Aquila. *Bulletin of Earthquake Engineering*, *9*(3), 741–759. https://doi.org/10.1007/s10518-011-9246-6

Milana, G., Cultrera, G., Bordoni, P., Bucci, A., Cara, F., Cogliano, R., et al. (2020). Local site effects estimation at Amatrice (Central Italy) through seismological methods. *Bulletin of Earthquake Engineering*, *18*, 5713–5739. https://doi.org/10.1007/s10518-019-00587-3

Minato, S., Tsuji, T., Ohmi, S., & Matsuoka, T. (2012). Monitoring seismic velocity change caused by the 2011 Tohoku-oki earthquake using ambient noise records. *Geophysical Research Letters*, *39*, L09309. https://doi.org/10.1029/2012GL051405

Molnar, S., Cassidy, J. F., Castellaro, S., Cornou, C., Crow, H., Hunter, J. A., et al. (2018). Application of microtremor horizontal-to-vertical spectral ratio (MHVSR) analysis for site characterization: State of the art. *Surveys in Geophysics*, *39*, 613–631. https://doi.org/10.1007/s10712-018-9464-4

Moretti, M., Pondrelli, S., Margheriti, L., Abruzzese, L., Anselmi, M., Arroucau, P., et al. (2017). Sismiko: Emergency network deployment and data sharing for the 2016 central Italy seismic sequence. *Annals of Geophysics*, *59*, Fast Track 5. https://doi.org/10.4401/ag-7212

Nakamura, Y. (1989). A method for dynamic characteristics estimation of subsurface using microtremor on the ground surface. *Quaterly Report of the Railway Technical Research Institue*, *30*(1), 25–30.

Nakamura, Y. (2019). What is the Nakamura method? *Seismological Research Letters*, *90*(4), 1437–1443. https://doi.org/10.1785/0220180376

Nakata, N., & Snieder, R. (2011). Near-surface weakening in Japan after the 2011 Tohoku-Oki earthquake. *Geophysical Research Letters*, *38*, L17302. https://doi.org/10.1029/2011GL048800

Nogoshi, M., & Igarashi, T. (1971). On the amplitude characteristics of microtremor (part 2) (in Japanese with English abstract). *Journal of seismological Society of Japan*, *24*, 26–40.

Olivier, G., Brenguier, F., Campillo, M., Roux, P., Shapiro, N. M., & Lynch, R. (2015). Investigation of coseismic and postseismic processes using in situ measurements of seismic velocity variations in an underground mine. *Geophysical Research Letters*, *42*, 9261–9269. https://doi.org/10.1002/2015GL065975

Pagliaroli, A., Pergalani, F., Ciancimino, A., Chiaradonna, A., Compagnoni, M., deSilva, F., et al. (2019). Site response analyses for complex geological and morphological conditions: Relevant case-histories from 3rd level seismic microzonation in central Italy. *Bulletin of Earthquake Engineering*, 1–37.

Parolai, S., Richwalski, S. M., Milkereit, C., & Bormann, P. (2004). Assessment of the stability of H/V spectral ratios from ambient noise and comparison with earthquake data in the Cologne area (Germany). *Tectonophysics*, *390*(1–4), 57–73.

Pei, S., Niu, F., Ben-Zion, Y., Sun, Q., Liu, Y., Xue, X., et al. (2019). Seismic velocity reduction and accelerated recovery due to earthquakes on the Longmenshan fault. *Nature Geoscience*, *12*, 387–392. https://doi.org/10.1038/s41561-019-0347-1

Peterson, J. (1993). Observation and modeling of seismic background noise. Open-File Rept. 93-322. *U.S. Geological Survey*, 94.

Picozzi, M., Parolai, S., & Albarello, D. (2005). Statistical analysis of noise horizontal-to-vertical spectral ratios (HVSR). *Bulletin of the Seismological Society of America*, *95*(5), 1779–1786.

Piña-Flores, J., Perton, M., García-Jerez, A., Carmona, E., Luzón, F., Molina-Villegas, J. C., & Sánchez-Sesma, F. J. (2016). The inversion of spectral ratio H/V in a layered system using the diffuse field assumption (DFA). *Geophysical Journal International*, ggw416.

Poli, P., Marguin, V., Wang, Q., D'Agostino, N., & Johnson, P. (2020). Seasonal and coseismic velocity variation in the region of L'Aquila from single station measurements and implications for crustal rheology. *Journal of Geophysical Research: Solid Earth*, *125*, e2019JB019316. https://doi.org/10.1029/2019JB019316

Priolo, E., Pacor, F., Spallarossa, D., Milana, G., Laurenzano, G., Romano, M. A., et al. (2020). Seismological analyses of the seismic microzonation of 138 municipalities damaged by the 2016–2017 seismic sequence in Central Italy. *Bulletin of Earthquake Engineering*, *18*(12), 5553–5593. https://doi.org/10.1007/s10518-019-00652-x

Rossi, A., Tertulliani, A., Azzaro, R., Graziani, L., Rovida, A., Maramai, A., et al. (2019). The 2016–2017 earthquake sequence in Central Italy: Macroseismic survey and damage scenario through the EMS-98 intensity assessment. *Bulletin of Earthquake Engineering*, *17*(5), 2407–2431. https://doi.org/10.1007/s10518-019-00556-w

Russo, E., Felicetta, C., D'Amico, M., Sgobba, S., Lanzano, G., Mascandola, C., et al. (2022). *Italian Accelerometric Archive v3.2 - Istituto Nazionale di Geofisica e Vulcanologia, Dipartimento della Protezione Civile Nazionale*. https://doi.org/10.13127/itaca.3.2

Sánchez-Sesma, F. J. (2017). Modeling and inversion of the microtremor H/V spectral ratio: Physical basis behind the diffuse field approach. *Earth Planets and Space*, *69*(1), 1–9.

Sánchez-Sesma, F. J., Rodríguez, M., Iturrarán-Viveros, U., Luzón, F., Campillo, M., Margerin, L., et al. (2011). A theory for microtremor H/V spectral ratio: Application for a layered medium. *Geophysical Journal International*, *186*(1), 221–225. https://doi.org/10.1111/j.1365-246X.2011.05064.x

Sawazaki, K., Sato, H., Nakahara, H., & Nishimura, T. (2006). Temporal change in site response caused by earthquake strong motion as revealed from coda spectral ratio measurement. *Geophysical Research Letters*, *33*(21), L21303. https://doi.org/10.1029/2006GL027938

Sawazaki, K., Sato, H., Nakahara, H., & Nishimura, T. (2009). Time-lapse changes of seismic velocity in the shallow ground caused by strong ground motion shock of the 2000 Western-Tottori Earthquake, Japan, as revealed from coda deconvolution analysis. *Bulletin of the Seismological Society of America*, *99*, 352–366.

SESAME. (2005). Guidelines for the implementation of the H/V spectral ratio technique on ambient vibrations: Measurements, processing and interpretation. *WP12-Deliverable D23*, *12*, 62.

Strollo, A., Cambaz, D., Clinton, J., Danecek, P., Evangelidis, C. P., Marmureanu, A., et al. (2021). Eida: The European integrated data archive and service infrastructure within ORFEUS. *Seismological Society of America*, *92*(3), 1788–1795.

Tertulliani, A., Arcoraci, L., Berardi, M., Bernardini, F., Camassi, R., Castellano, C., et al. (2011). An application of EMS98 in a medium-sized city: The case of L'aquila (central Italy) after the April 6, 2009 Mw 6.3 earthquake. *Bulletin of Earthquake Engineering*, *9*(1), 67–80.

Wathelet, M., Chatelain, J. L., Cornou, C., Giulio, G. D., Guillier, B., Ohrnberger, M., & Savvaidis, A. (2020). Geopsy: A user-friendly open-source tool set for ambient vibration processing. *Seismological Research Letters*, *91*(3), 1878–1889. https://doi.org/10.1785/0220190360

Wegler, U., & Sens-Schönfelder, C. (2007). Fault zone monitoring with passive image interferometry. *Geophysical Journal International*, *168*(3), 1029–1033. https://doi.org/10.1111/j.1365-246X.2006.03284.x

Working group INGV. (2018a). Geological report at the seismic station IV.NRCA–Norcia (PG). *Agreement DPC-INGV 2018, allegato B2, obiettivo 1 - TASK B*. https://doi.org/10.5281/zenodo.2430497

Working group INGV. (2018b). Velocity profile report at the seismic station IV.NRCA-NORCIA. *Agreement DPC-INGV 2018, allegato B2, obiettivo 1 - TASK B*. https://doi.org/10.5281/zenodo.2358257

Wu, C., & Peng, Z. (2011). Temporal changes of site response during the 2011 M_w 9.0 off the Pacific coast of Tohoku Earthquake. *Earth Planets and Space*, *63*, 51. https://doi.org/10.5047/eps.2011.06.011

Wu, C., & Peng, Z. (2012). Long-term change of site response after the Mw 9.0 Tohoku earthquake in Japan. *Earth Planets and Space*, *64*(12), 1259–1266. https://doi.org/10.5047/eps.2012.05.012

Wu, C., Peng, Z., & Ben-Zion, Y. (2009). Non-linearity and temporal changes of fault zone site response associated with strong ground motion. *Geophysical Journal International*, *176*(1), 265–278.

Yukutake, Y., Ueno, T., & Miyaoka, K. (2016). Determination of temporal changes in seismic velocity caused by volcanic activity in and around Hakone volcano, central Japan, using ambient seismic noise records. *Progress in Earth and Planetary Science*, *3*(1), 29. https://doi.org/10.1186/s40645-016-0106-5